Disk-shaped Bose–Einstein condensates in the presence of an harmonic trap and an optical lattice

Todd Kapitula,[1,a)] Panayotis G. Kevrekidis,[2,b)] and D. J. Frantzeskakis[3,c)]
[1]*Department of Mathematics and Statistics, Calvin College, Grand Rapids, Michigan 49456, USA*
[2]*Department of Mathematics and Statistics, University of Massachusetts, Amherst, Massachusetts 01003-4515, USA*
[3]*Department of Physics, University of Athens, Panepistimiopolis, Zografos, Athens 15784, Greece*

(Received 12 November 2007; accepted 22 February 2008; published online 9 April 2008)

We study the existence and stability of solutions of the two-dimensional nonlinear Schrödinger equation in the combined presence of a parabolic and a periodic potential. The motivating physical example consists of Bose–Einstein condensates confined in an harmonic (e.g., magnetic) trap and an optical lattice. By connecting the nonlinear problem with the underlying linear spectrum, we examine the bifurcation of nonlinear modes out of the linear ones for both focusing and defocusing nonlinearities. In particular, we find real-valued solutions (such as multipoles) and complex-valued ones (such as vortices). A primary motivation of the present work is to develop "rules of thumb" about what waveforms to expect emerging in the nonlinear problem and about the stability of those modes. As a case example of the latter, we find that among the real-valued solutions, the one with larger norm for a fixed value of the chemical potential is expected to be unstable. © *2008 American Institute of Physics*. [DOI: 10.1063/1.2897311]

Herein, we consider the existence and stability of weakly nonlinear solutions of a nonlinear Schrödinger equation with a harmonic and a periodic potential in two space dimensions. The form of the potential is motivated from the dynamics of Bose–Einstein condensates in the presence of a magnetic trap and optical lattice. We use Lyapunov–Schmidt theory to rigorously establish the existence of multipoles and vortices in the presence of attractive and repulsive nonlinear interparticle interactions. When considering the spectral stability of these nonlinear solutions, we use another Lyapunov–Schmidt analysis to develop a "rule of thumb" to determine which of the multipoles are dynamically unstable. The results are corroborated with numerical computations.

I. PHYSICAL MOTIVATION

In the past few years, there has been a tremendous focus of research effort on the study of Bose–Einstein condensates (BECs).[1,2] This context has provided a wide array of interesting phenomena, not only because of the very precise experimental control that exists over the relevant setups,[3] but also because of the exciting connections that the field opens with other areas of physics such as nonlinear optics and wave theory. This is to a large extent due to the very efficient mean-field description of BECs, based on a classical nonlinear evolution equation of the nonlinear Schrödinger type; namely, the Gross–Pitaevskii (GP) equation.[1–3]

The main novel feature offered in the context of the current experimental realizations is the unprecedented control over the external potentials that are used to confine the ultracold bosonic atoms. In particular, such confinement is primarily harmonic, and was first implemented by magnetic fields and later by optical fields as well; this type of confinement is very accurately modeled by a parabolic potential at the GP level. Optical fields are also used for the creation of a periodic confining potential known as "optical lattice." The latter is generated by counterpropagating laser beams whose interference produces the desired potential, and is modeled by trigonometric periodic potentials in the GP equation. Relevant reviews concerning the above features, and discussing the dynamics of BECs, as well as the coherent nonlinear structures arising in them, have already appeared. These include extensive studies on bright solitons in BECs,[4] vortices in BECs,[5,6] instabilities in BECs,[7] hydrodynamic/kinetic theory aspects of the superfluid dynamics,[8] and, finally, the behavior of BECs in optical lattice potentials.[9,10] Inasmuch as the study of matter waves in BECs is an extremely active area of research for which new books[11] and reviews[12] continue to emerge, we should alert the interested reader that this list is meant to be representative rather than exhaustive.

It is well known that the effective nonlinearity, which is induced by the interparticle interactions, sustains the existence of a variety of macroscopic nonlinear structures in the form of matter-wave solitons which, importantly, have been observed in experiments. These include bright solitons[13] for attractive interactions (focusing nonlinearity in the GP equation), and dark solitons,[14] as well as gap solitons,[15] for repulsive interactions (defocusing nonlinearity in the GP equation). One technique that has been perhaps slightly less used (as compared to purely nonlinear dynamics techniques) for the study of such structures relies on the continuation of

a)Electronic mail: tmk5@calvin.edu; URL: http://www.calvin.edu/~tmk5.
b)Electronic mail: kevrekid@math.umass.edu; URL: http://www.math.umass.edu/~kevrekid.
c)Electronic mail: dfrantz@phys.uoa.gr; URL: www.phys.uoa.gr/el-lab/cv/frantzeskakis.html.

linear states into nonlinear ones. This idea has been explored at the level of the respective stationary problem for one-dimensional and higher-dimensional (and particularly radially symmetric) states in the presence of harmonic trapping (see, e.g., Refs. 16–18 and references therein). On the other hand, the dynamics of such nonlinear states arising from the continuation of their linear counterparts has been explored through the so-called Feshbach resonance management technique, which allows the temporal variation of the nonlinearity.[19] Finally, the same idea has also been explored in the one-dimensional case from the point of view of bifurcation and stability theory (see, e.g., Ref. 20). All of the above studies were either at the level of one dimension or at the level of multidimensions, but in the presence of an harmonic trap only.

Our aim in the present work is to expand the analysis presented in Ref. 20 to the two-dimensional setting. We will provide a perturbative characterization of the nonlinear existence and stability problem from the linear limit for BECs under magnetic and optical confinement. One of our goals is to provide general rules of thumb for the characterization of the types of states that bifurcate from the linear limit and of their corresponding stability. In addition to the general features, we provide a detailed analysis. In the case of the existence problem this determines the approximate nonlinear solution profiles, which to leading order are appropriate linear combinations of the linear states. In the case of the spectral stability problem, it allows us to evaluate the bifurcation of both $\mathcal{O}(\epsilon)$, where ϵ represents the strength of the nonlinearity, and $\mathcal{O}(1)$ eigenvalues, which may lead to instability through real pairs or complex quartets.

Our presentation is structured as follows. In Sec. II we give the general mathematical framework of the problem and some of the main theoretical conclusions. In Sec. III we present some motivating numerical examples showcasing the validity of our findings. We will then determine the existence (Sec. IV) and stability (Secs. V and VI) of the solutions of the nonlinear two-dimensional problem that emerge from the linear limit. Finally, in Sec. VII we briefly summarize our results.

II. MATHEMATICAL SETUP AND MAIN RESULTS

Consider the following GP mean-field model for a disk-shaped (quasi-two-dimensional) BEC confined in both an harmonic (e.g., magnetic) trap and an optical lattice (see, e.g., Ref. 7 for the derivation and details on the normalizations):

$$iq_t + \tfrac{1}{2}\Delta q + \omega q + a|q|^2 q = (\tfrac{1}{2}\Omega[x^2+y^2] + V_0[p(x)+p(y)])q, \tag{2.1}$$

where $a \in \{-1,+1\}$ is positive (negative) for attractive (repulsive) interatomic interactions, $\omega \in \mathbb{R}$ is the chemical potential, $\Omega \in \mathbb{R}^+$ represents the strength of the magnetic trap, $V_0 \in \mathbb{R}$ represents the strength of the optical lattice, and $p(\cdot):\mathbb{R}\mapsto\mathbb{R}$ is L-periodic and even and is a model for the optical lattice; finally, q represents the condensate's mean-field wavefunction. The above GP equation can be rescaled in the so-called harmonic oscillator units, so that the strength of the magnetic trap is independent of Ω. Thus, rescaling the variables of Eq. (2.1) as

$$\tilde{x} := \sqrt{\Omega}x, \quad \tilde{y} := \sqrt{\Omega}y, \quad \tilde{t} := \Omega t, \quad \tilde{\omega} := \frac{\omega}{\Omega}, \quad \tilde{q} := \frac{q}{\sqrt{\Omega}}, \tag{2.2}$$

and dropping the tildes, the following equation is obtained:

$$iq_t + \frac{1}{2}\Delta q + \omega q + a|q|^2 q = \left[\frac{1}{2}(x^2+y^2) + \frac{V_0}{\Omega}\left(p\left(\frac{x}{\sqrt{\Omega}}\right) + p\left(\frac{y}{\sqrt{\Omega}}\right)\right)\right]q. \tag{2.3}$$

Notice that in the above formulation if $0<\Omega\ll 1$, then the optical lattice is rapidly varying with respect to the magnetic trap. Furthermore, it is noted that once a solution $\tilde{q}(\tilde{x},\tilde{y},\tilde{t})$ to Eq. (2.3) has been found, the solution to Eq. (2.1) is recovered by

$$q(x,t) = \sqrt{\Omega}\tilde{q}\left(\sqrt{\Omega}x, \sqrt{\Omega}y, \Omega t\right).$$

It should also be mentioned here that the above mean-field model is applicable for sufficiently weak optical lattices. For strong optical lattices, quantum fluctuations become relevant and the system enters into the Mott-insulating phase,[21] which invalidates the assumptions of the mean-field description leading to the GP equation discussed herein.

The goal of this paper is to consider the existence and spectral stability of small solutions to Eq. (2.3). In particular, we will consider steady-state solutions of the form

$$Q = (x_1 q_{j,k} + y_1 q_{k,j} + iy_2 q_{k,j})\epsilon^{1/2} + \mathcal{O}(\epsilon),$$

where $x_1, y_1, y_2 \in \mathbb{R}$ and $q_{m,n}$ is an eigenfunction for the linear problem that has the property that there are m vertical nodal lines and n horizontal nodal lines [see also Eq. (4.3)]. The particular values of x_1, y_1, and y_2 depend implicitly upon the trap parameters V_0 and Ω, as well as whether $j+k$ is odd or even (see Sec. IV). The formal small parameter ϵ characterizes the size of the deviation from the linear limit in our weakly nonlinear analysis. The following result will be shown:

Proposition II.1: *There exist two distinct steady-state real-valued solutions to Eq. (2.3) for $\epsilon>0$ sufficiently small*:

(a) $Q = x_1(q_{j,k}+q_{k,j})\epsilon^{1/2}+\mathcal{O}(\epsilon)$, *where x_1 is given in Eq. (4.10)*;

(b) $Q = \rho(\cos\varphi\, q_{j,k} + \sin\varphi\, q_{k,j})\epsilon^{1/2}+\mathcal{O}(\epsilon)$, *where ρ,φ are given in Eq. (2.3) ($\varphi=0$ if $j+k$ is odd).*

There exists one distinct steady-state complex-valued solution to Eq. (2.3) for $\epsilon>0$ sufficiently small:

$$Q = \rho(q_{j,k} + e^{i\varphi}q_{k,j})\epsilon^{1/2} + \mathcal{O}(\epsilon),$$

where (ρ,φ) is given in Eq. (4.18) ($\varphi=\pi/2$ if $j+k$ is odd). For all of the solutions, the chemical potential satisfies $\omega\sim\lambda_{j,k}+\omega_p\epsilon$ with $a\omega_p<0$, where $\lambda_{j,k}$ is defined in Eq. (4.2).

Remark II.2: If the optical lattice is not present, then there will be only one distinct real-valued solution, and all other real-valued solutions will be related via the **SO**(2) spatial rotation symmetry. The lattice acts as a symmetry-

breaking term that preserves the discrete $\mathbf{D}_4$ square symmetry; hence, the existence of the second distinct solution.

Once the existence of these small waves has been determined via a Lyapunov–Schmidt reduction, we consider the problem of determining the spectrum for the appropriate linear operator. There will be two sets of eigenvalues to consider:

(a) the $\mathcal{O}(\epsilon)$ eigenvalues which arise from the reduction;
(b) the $\mathcal{O}(1)$ eigenvalues that may possibly lead to oscillatory instabilities via a Hamiltonian–Hopf bifurcation.

We completely characterize the location of the $\mathcal{O}(\epsilon)$ eigenvalues analytically (see Sec. V), and we find that:

(a) if $j+k$ is odd, then the real-valued solution with the larger number of particles for a fixed value of the chemical potential is unstable, whereas the other one is spectrally stable [at least with respect to the $\mathcal{O}(\epsilon)$ eigenvalues];
(b) if $j+k$ is odd, then the complex-valued solution is spectrally stable [at least with respect to the $\mathcal{O}(\epsilon)$ eigenvalues];
(c) if $j+k$ is even, then there is numerical evidence to support the conclusions of (a) and (b).

We will only briefly discuss the unstable eigenvalues that can be created via the Hamiltonian–Hopf bifurcation (see Sec. VI). Regarding the $\mathcal{O}(1)$ eigenvalues, we find that the complex-valued solution will be spectrally unstable if the ratio V_0/Ω lies in the *HH vortex resonance band*. Otherwise, our analysis is inconclusive, and we need to numerically determine the spectrum (see Sec. III for an example).

III. NUMERICAL EXAMPLES

In this section we numerically show a motivational illustration of the most fundamental case among the ones discussed in this work; namely, the one with $(j,k)=(0,1)$. As discussed in Proposition II.1, two distinct real solutions emerge from the linear limit; namely, the mode involving $Q\sim q_{1,0}\epsilon^{1/2}$ (related to $q_{0,1}\epsilon^{1/2}$ via the discrete $\mathbf{D}_4$ square symmetry) and the one involving $Q\sim(q_{1,0}+q_{0,1})\epsilon^{1/2}$. These modes are related by $\mathbf{SO}(2)$ rotation symmetry in the limit of $V_0=0$, but become distinct for $V_0\neq 0$. This relationship is clearly shown in panels (A)–(D) of Fig. 1, which show the modes for $V_0=0$ and $V_0=0.5$. Figure 2 reveals their respective stability properties by showing the eigenvalues with nonzero real parts (top panels of Fig. 1) as well as the squared L^2-norm, physically associated with the number of atoms in the BEC (bottom panels of Fig. 1). Additionally, in panels (E)–(H), we also show a complex-valued solution $Q\sim(q_{1,0}+iq_{0,1})\epsilon^{1/2}$ representing a vortex[5,6] that is always found to be spectrally stable.

Regarding the stability of the two real states, we note that as indicated above the state $Q\sim q_{1,0}\epsilon^{1/2}$, which has the larger norm (see the bottom panel of stability in Fig. 2), is indeed the one which is always unstable due to a real eigenvalue pair (see the top right panel of stability in Fig. 2). Additionally, that solution possesses the interesting feature, illustrated in the top left panels of stability, that a second

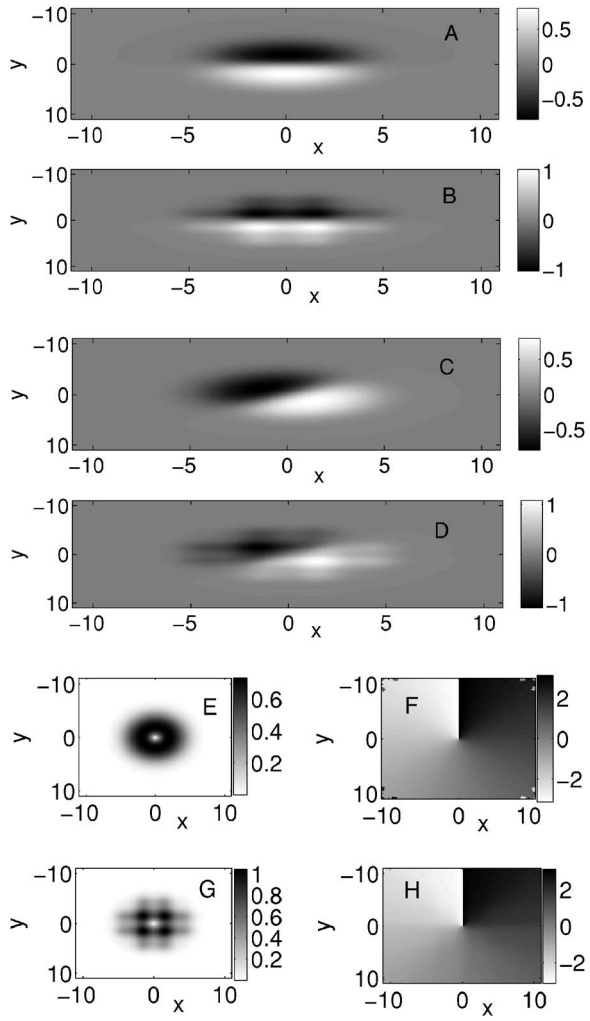

FIG. 1. Panels A and B show the solution proportional to $q_{1,0}$ for $V_0=0$ and $V_0=0.5$, respectively. Panels C and D show the same features for the second distinct real mode; namely, the one proportional to $q_{1,0}+q_{0,1}$. The bottom panels show the modulus (panels E and G) and phase (panels F and H) of the vortex configuration proportional to $q_{1,0}+iq_{0,1}$. These profiles have been obtained for parameter values $\Omega=0.3$ and $\omega=1$ and for a defocusing nonlinearity ($a=-1$); profiles pertaining to the focusing nonlinearity ($a=+1$) have also been similarly obtained.

unstable eigenmode arises due to an eigenvalue quartet for $0.05<V_0<0.15$, while for $V_0>0.17$, one of the two pairs of the quartet becomes real constituting a secondary instability that eventually becomes the dominant mode, for sufficiently large V_0; this justifies the presence of two modes in panel A of stability. On the other hand, as predicted, the solution $Q\sim(q_{1,0}+q_{0,1})\epsilon^{1/2}$ is stable for small V_0. However, for $0.09<V_0<0.39$, it becomes unstable due to a complex eigenvalue quartet stemming from the collision of two pairs on the imaginary axis; in fact, a second such quartet emerges for $0.3<V_0<0.38$. The bifurcation of these two quartets (both as a function of V_0 and as a case example for $V_0=0.35$) is shown in panels (d) and (e) of Fig. 2.

Finally, we have also investigated the dynamics of these unstable solutions when evolved according to the original Eq. (2.1). In particular, in Fig. 3, the evolution of the solution proportional to $q_{1,0}$ for $V_0=0.1$ and $V_0=0.5$ (top and middle panels of the figure, respectively), and of the solution pro-

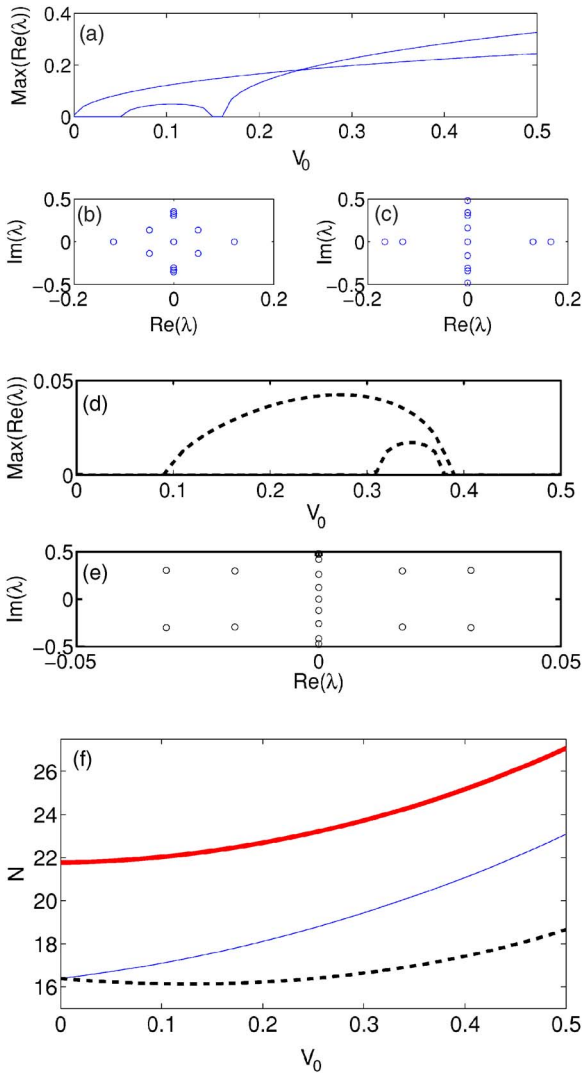

FIG. 2. (Color online) Panel (a) shows the dependence of the most unstable eigenvalues' real part on V_0 (top), while panels (b) and (c) show two typical examples of the spectral planes for $V_0=0.1$ and $V_0=0.2$, respectively, for the solution proportional to $q_{1,0}$. Panels (d) and (e) show corresponding features for the solution proportional to $q_{1,0}+q_{0,1}$ [the spectral plane in panel (e) is shown for $V_0=0.35$]. Finally, panel (f) shows the squared L^2 norms (proportional to the number of atoms) for the two real (thin solid and dashed lines) and the one complex (thick solid line) modes.

portional to $q_{1,0}+iq_{0,1}$ for $V_0=0.25$ (bottom panel) is shown. In all the cases, we observe that the instability eventually destroys the configuration leading to an oscillatory behavior. It can be noted that the time that it takes for the perturbations to manifest the instability is larger, the smaller the instability growth rate. Furthermore, in the evolution with $V_0=0.1$, the optical lattice is fairly weak and the breakup dynamics (leading to alternations of the high density region) seem to have a rotational character whereby these regions rotate around the center of the condensate. This is not so in the case of the strong lattice for $V_0=0.5$, where the oscillatory density dynamics is present, but any rotation is absent. Finally, in the bottom panel oscillatory dynamics between the two high density lobes of the $q_{1,0}+iq_{0,1}$ solution is also observed.

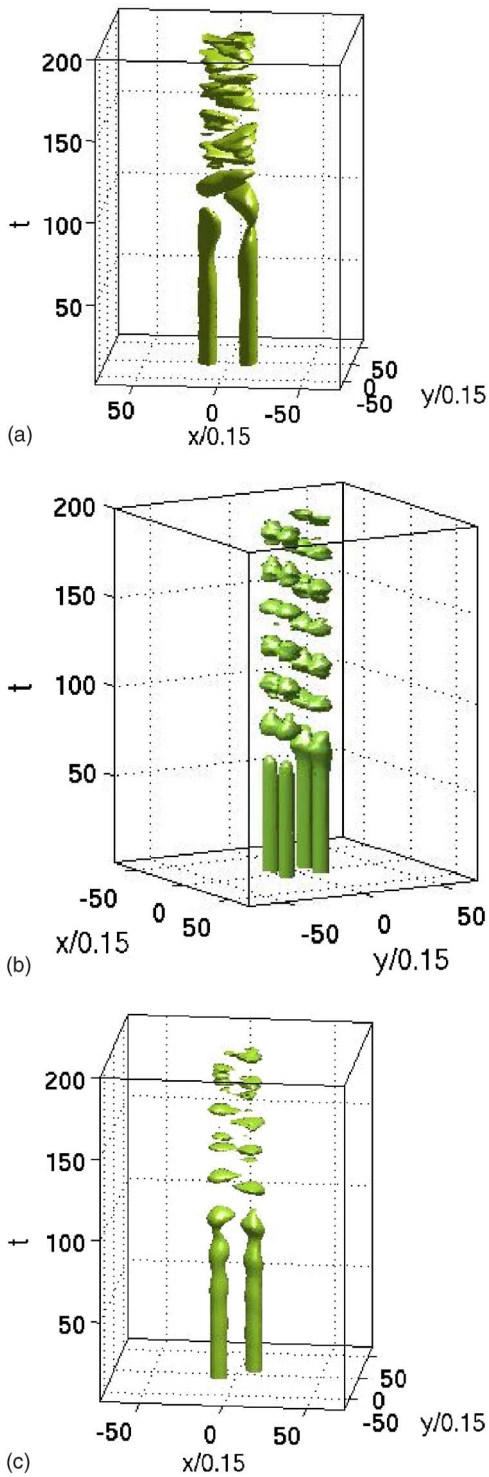

FIG. 3. (Color online) Panel (a) shows the space-time evolution of a typical contour of the solution proportional to $q_{1,0}$ for $V_0=0.1$. Panel (b) shows the same but for the case with $V_0=0.5$, while panel (c) shows the solution proportional to $q_{1,0}+q_{0,1}$ spatiotemporally evolving for the case with $V_0=0.25$. These results are for the same solution parameters, $\Omega=0.3$ and $\omega=1$ and $a=-1$, as used in profiles.

IV. EXISTENCE OF NONLINEAR SOLUTIONS

A. The eigenvalue problem

In order to apply the Lyapunov–Schmidt reduction to find nonlinear solutions in the case of weak nonlinearity, one must first understand the spectrum $\sigma(\mathcal{L})$ of the operator $\mathcal{L} := \mathcal{L}_x+\mathcal{L}_y$, where for $\alpha \in \{x,y\}$

$$\mathcal{L}_\alpha := -\frac{1}{2}\partial_\alpha^2 - \omega_\alpha + \frac{1}{2}\alpha^2 + \frac{V_0}{\Omega}p\left(\frac{\alpha}{\sqrt{\Omega}}\right). \tag{4.1}$$

Since $\mathcal{L}$ is the sum of one-dimensional Schrödinger operators, by using separation of variables one deduces that if $\lambda_\alpha \in \sigma(\mathcal{L}_\alpha)$ with associated eigenfunction q_α, then $\lambda_x+\lambda_y \in \sigma(\mathcal{L})$ with associated eigenfunction $q_x(x)q_y(y)$. Thus, it is sufficient to consider the operators $\mathcal{L}_\alpha$. A study of these operators was done in Ref. 20, from which one can deduce the following:

(a) $\sigma(\mathcal{L}_\alpha)$ is solely composed of point spectrum, and each eigenvalue is simple;
(b) the eigenfunctions form a complete orthonormal basis;
(c) each eigenfunction $q_{n,\alpha}(\alpha)$ satisfies the decay condition

$$|q_{n,\alpha}(\alpha)|e^{\alpha^2/8} \leqslant C, \quad \alpha \in \mathbb{R}.$$

Let us order the simple eigenvalues of $\mathcal{L}_\alpha$ as $\lambda_{0,\alpha}<\lambda_{1,\alpha}<\cdots$, and denote the associated eigenfunctions by $q_{j,\alpha}(\cdot)$. Since $p(\cdot)$ is even, one has that $q_{j,\alpha}(\cdot)$ is even if j is even, and is odd if j is odd.

As will be further discussed in Sec. IV, it is of interest to determine those solutions which arise from the linear limit in which an eigenvalue has multiplicity 2 (see Ref. 22 for the case of eigenvalues with multiplicity 3). As stated above, the eigenvalues of $\mathcal{L}$ are given by

$$\lambda_{j,k} := \lambda_{j,x} + \lambda_{k,y}, \tag{4.2}$$

and the associated eigenfunction is given by

$$q_{j,k}(x,y) := q_{j,x}(x)q_{k,y}(y). \tag{4.3}$$

In order for an eigenvalue to be semi-simple, one then requires that

$$\lambda_{j,k} = \lambda_{j',k'}$$

for some $(j',k') \neq (j,k)$. Such a scenario easily arises, for $\lambda_{j,k}=\lambda_{k,j}$ for any pair of $j,k \in \mathbb{N}_0$ with $j \neq k$.

B. The Lyapunov–Schmidt reduction

If the eigenvalue is simple, then a straightforward application of the Lyapunov–Schmidt reduction yields that there is a small nonlinear solution of the form

$$Q_{j,k}(x,y) = \epsilon q_{j,k}(x,y) + \mathcal{O}(\epsilon^2)$$

for ω chosen so that $\omega=\lambda_{j,k}+\mathcal{O}(\epsilon)$ (Ref. 23, Chap. 7). Furthermore, it can be shown that the bifurcation is subcritical if $a=+1$, and is supercritical if $a=-1$ (see Sec. IV of Ref. 20).

The interest herein will be the case that the geometric multiplicity of the eigenvalue is 2. Note that Eq. (2.3) is invariant under the actions

$$(q;x,y) \mapsto (-q;x,y), \quad (q;x,y) \mapsto (q;-x,y),$$

$$(q;x,y) \mapsto (q;x,-y);$$

thus, the bifurcation equations derived via the Lyapunov–Schmidt procedure will have a $(\mathbb{Z}_2 \oplus \mathbb{Z}_2)$-symmetry. Furthermore, one has the gauge symmetry $q \mapsto qe^{i\theta}$. As noted in Sec. IV A, one has that $\lambda_{j,k}=\lambda_{k,j}$ for any $j,k \epsilon \mathbb{N}_0$. It will henceforth be assumed in this section that $\lambda_{j',k'} \neq \lambda_{j,k}$ for $(j',k') \notin \{(j,k),(k,j)\}$. Following the ideas presented in Ref. 22, choose ω so that the nonlinear solution can be written as

$$\begin{aligned} Q &= (x_1 q_{j,k} + y_1 q_{k,j} + iy_2 q_{k,j})\epsilon^{1/2} + \mathcal{O}(\epsilon), \\ \omega &= \lambda_{j,k} + \omega_p \epsilon + \mathcal{O}(\epsilon^{3/2}), \end{aligned} \tag{4.4}$$

where $x_1,y_1,y_2 \in \mathbb{R}$. Here the gauge symmetry is being implicitly used. Set $\mu := a\omega_p$. Upon using the Lyapunov–Schmidt reduction, and the fact that $q_{j,x}(\cdot)=q_{j,y}(\cdot)$, one sees that the bifurcation equations are given by

$$\begin{aligned} 0 &= x_1[\mu + Ax_1^2 + B(3y_1^2 + y_2^2)] + Cy_1[3x_1^2 + y_1^2 + y_2^2], \\ 0 &= y_1[\mu + A(y_1^2 + y_2^2) + 3Bx_1^2] + Cx_1[x_1^2 + 3y_1^2 + y_2^2], \\ 0 &= y_2[\mu + A(y_1^2 + y_2^2) + Bx_1^2 + 2Cx_1y_1]. \end{aligned} \tag{4.5}$$

The coefficients in Eq. (4.5) are given by

$$A := g_{jjjj}g_{kkkk}, \quad B := (g_{jjkk})^2, \quad C := g_{jjjk}g_{jkkk}, \tag{4.6}$$

where

$$g_{ijk\ell} := \int_{-\infty}^{+\infty} q_{i,x}q_{j,x}q_{k,x}q_{\ell,x}dx.$$

Note that Eq. (4.5) inherits the $(\mathbb{Z}_2 \oplus \mathbb{Z}_2)$-symmetry via the invariances

$$(x_1,y_1,y_2) \mapsto (-x_1,-y_1,y_2), \quad (x_1,y_1,y_2) \mapsto (x_1,y_1,-y_2).$$

Further note that since $p(\cdot)$ is even, if $j+k=2\ell+1$ for some $\ell \in \mathbb{N}_0$, then $C=0$. Finally note that $A,B \in \mathbb{R}^+$, whereas the sign of C is indeterminate.

C. Real-valued solutions

Suppose that $y_2=0$. Upon setting

$$x_1 := \rho\cos\varphi, \quad y_1 := \rho\sin\varphi, \tag{4.7}$$

Eq. (4.5) becomes

$$\begin{aligned} 0 &= \cos\varphi[\mu + A\rho^2\cos^2\varphi + 3B\rho^2\sin^2\varphi] \\ &\quad + C\sin\varphi(2+\cos 2\varphi)\rho^2, \\ 0 &= \sin\varphi[\mu + A\rho^2\sin^2\varphi + 3B\rho^2\cos^2\varphi] \\ &\quad + C\cos\varphi(2-\cos 2\varphi)\rho^2. \end{aligned} \tag{4.8}$$

In turn, upon using the appropriate trigonometric identities Eq. (4.8) can be rewritten as

$$\begin{aligned} 0 &= \cos 2\varphi[\mu + (A + C\sin 2\varphi)\rho^2], \\ 0 &= \mu + \tfrac{1}{2}[A(2-\sin^2 2\varphi) + 3B\sin^2 2\varphi + 2C\sin 2\varphi]\rho^2. \end{aligned} \tag{4.9}$$

First suppose that $\cos 2\varphi=0$ in Eq. (4.9). One then has that

$$\rho^2 = -\frac{2\mu}{A+3B\pm 4C},$$

which from Eq. (4.7) yields the solutions

$$x_1^2 = y_1^2 = -\frac{\mu}{A + 3B \pm 4C}. \tag{4.10}$$

Now suppose that $\cos 2\varphi \neq 0$. One then has that

$$\rho^2 \sin 2\varphi[(A-3B)\sin 2\varphi - 2C] = 0.$$

If $\sin 2\varphi = 0$, then an examination of Eq. (4.8) shows that one gets a valid solution if and only if $C=0$. Otherwise, one necessarily has that

$$\sin 2\varphi = \frac{2C}{A-3B}, \quad \rho^2 = -\frac{\mu}{A + C\sin 2\varphi}. \tag{4.11}$$

Note that if $C=0$, then Eq. (4.11) reduces to

$$(x_1^2, y_1^2) = \left(-\frac{\mu}{A}, 0\right), \quad (x_1^2, y_1^2) = \left(0, -\frac{\mu}{A}\right) \quad (C=0). \tag{4.12}$$

D. Complex-valued solutions

Now suppose that $y_2 \neq 0$. Upon setting

$$y_1 := \rho\cos\varphi, \quad y_2 := \rho\sin\varphi, \tag{4.13}$$

Eq. (4.5) becomes

$$\begin{aligned} 0 &= x_1[\mu + Ax_1^2 + B(2+\cos 2\varphi)\rho^2] + C\rho\cos\varphi[3x_1^2 + \rho^2], \\ 0 &= \rho\cos\varphi[\mu + A\rho^2 + 3Bx_1^2] + Cx_1[x_1^2 + (2+\cos 2\varphi)\rho^2], \\ 0 &= \mu + A\rho^2 + Bx_1^2 + 2Cx_1\rho\cos\varphi. \end{aligned} \tag{4.14}$$

Upon substituting the last equation in Eq. (4.14) into the second equation and simplifying, one sees that

$$\begin{aligned} 0 &= x_1[\mu + Ax_1^2 + B(2+\cos 2\varphi)\rho^2] + C\rho\cos\varphi[3x_1^2 + \rho^2], \\ 0 &= x_1[2Bx_1\rho\cos\varphi + C(x_1^2 + \rho^2)], \\ 0 &= \mu + A\rho^2 + Bx_1^2 + 2Cx_1\rho\cos\varphi. \end{aligned} \tag{4.15}$$

Now assume that $x_1 \neq 0$; otherwise, by the gauge invariance one is back to looking for real-valued solutions. Upon substituting the second equation of Eq. (4.15) into the first equation and simplifying, one gets

$$\begin{aligned} 0 &= x_1[\mu + Ax_1^2 + B\rho^2 + 2Cx_1\rho\cos\varphi], \\ 0 &= 2Bx_1\rho\cos\varphi + C(x_1^2 + \rho^2), \\ 0 &= \mu + A\rho^2 + Bx_1^2 + 2Cx_1\rho\cos\varphi. \end{aligned} \tag{4.16}$$

From Eq. (4.16), one now gets that

$$(A-B)(\rho^2 - x_1^2) = 0. \tag{4.17}$$

Since the Hölder inequality implies that $B \leqslant A$, and since generically the inequality is strict, one now sees that $\rho^2 = x_1^2$. Plugging this into the second equation of Eq. (4.16) and simplifying yields

$$\begin{aligned} &\cos\varphi = \mp\frac{C}{B} \quad (x_1 = \pm\rho), \\ &\rho^2 = -\frac{\mu}{A + B - 2|C\cos\varphi|}. \end{aligned} \tag{4.18}$$

Note that if $C=0$, then the solution becomes

$$(x_1^2, y_2^2, x_1^2) = -\frac{\mu}{A+B}(1,0,1) \quad (C=0). \tag{4.19}$$

V. STABILITY: SMALL EIGENVALUES

The theory leading to the determination of the spectral stability of the solutions found in Sec. IV will depend upon the results presented in [Ref. 22, Sec. 5.1] and Refs. 24–27. Upon taking real and imaginary parts via $q := u + iv$, and linearizing Eq. (2.3) about a complex-valued solution $Q = U + iV$, one has the eigenvalue problem

$$\boldsymbol{J}\mathcal{L}\boldsymbol{u} = \lambda\boldsymbol{u}, \tag{5.1}$$

where

$$\boldsymbol{J} := \begin{pmatrix} 0 & 1 \\ -1 & 0 \end{pmatrix}, \quad \mathcal{L} := (\mathcal{L}_0 - \omega)\mathbb{1} - a\begin{pmatrix} 3U^2 + V^2 & 2UV \\ 2UV & U^2 + 3V^2 \end{pmatrix},$$

and

$$\mathcal{L}_0 := -\frac{1}{2}(\partial_x^2 + \partial_y^2) + \frac{1}{2}(x^2 + y^2) + \frac{V_0}{\Omega}\left[p\left(\frac{x}{\sqrt{\Omega}}\right) + p\left(\frac{y}{\sqrt{\Omega}}\right)\right].$$

Consider the solutions described in Sec. IV. Since $U, V = \mathcal{O}(\sqrt{\epsilon})$, one has that in Eq. (5.1)

$$\mathcal{L} = (\mathcal{L}_0 - \lambda_{j,k})\mathbb{1} + \mathcal{O}(\epsilon).$$

Since by assumption $\dim[\ker(\mathcal{L}_0 - \lambda_{j,k})\mathbb{1}] = 4$, one has that for Eq. (5.1) there will be four eigenvalues of $\mathcal{O}(\epsilon)$. Two of these eigenvalues will remain at the origin due to the symmetries present in Eq. (2.3); in particular, the gauge symmetry, which leads to the conservation of the number of particles N, where

$$N := \int\int_{\mathbb{R}^2} |q(\boldsymbol{x})|^2\, d\boldsymbol{x}.$$

Consequently, there will only be two nonzero eigenvalues of $\mathcal{O}(\epsilon)$. Unfortunately, the perturbation calculations presented below will be insufficient to fully determine the spectral stability of the solutions, for it is possible that $\mathcal{O}(1)$ eigenvalues of opposite sign collide, and hence create a so-called oscillatory instability associated with a complex eigenvalue. This issue will be considered briefly in Sec. VI. The interested reader should also consult Sec. 6 of Ref. 22 and the references therein.

The determination of the $\mathcal{O}(\epsilon)$ eigenvalues can be found via a reduction to a finite-dimensional eigenvalue problem. To see this, consider Eq. (5.1) written in the form

$$\mathcal{J} := \begin{pmatrix} 0 & 1 \\ -1 & 0 \end{pmatrix}, \quad \mathcal{L} = \mathcal{A}_0 + \epsilon \mathcal{L}_\epsilon,$$

with

$$\mathcal{A}_0 := (\mathcal{L}_0 - \lambda_{j,k})\mathbb{1}, \quad \mathcal{L}_\epsilon := \begin{pmatrix} \mathcal{L}_+ & \mathcal{B} \\ \mathcal{B} & \mathcal{L}_- \end{pmatrix}. \tag{5.2}$$

Here it is assumed that $0<\epsilon\ll 1$, and that the operators $\mathcal{L}_\pm$ and $\mathcal{B}$ are self-adjoint on a Hilbert space H with inner product $\langle\cdot,\cdot\rangle$. Furthermore, it will be assumed that the operators satisfy the assumptions given in Sec. 2 of Ref. 24.

Assume that the orthonormal basis for $\ker(L_0)$ is given by

$$\ker(\mathcal{A}_0) = \mathrm{Span}\{\varphi_1, \varphi_2\}. \tag{5.3}$$

As seen in Ref. 28, Sec. 4, upon writing

$$\lambda = \epsilon\lambda_1 + \mathcal{O}(\epsilon^2), \quad u = \sum_{j=1}^{2} c_j(\varphi_j, 0)^{\mathrm{T}} + \sum_{j=1}^{2} c_{2+j}(0, \varphi_j)^T + \mathcal{O}(\epsilon),$$

the determination of the $\mathcal{O}(\epsilon)$ eigenvalues to Eq. (5.2) is equivalent to the finite-dimensional eigenvalue problem

$$\boldsymbol{JSx} = \lambda_1 \boldsymbol{x}; \quad \boldsymbol{J} := \begin{pmatrix} \boldsymbol{0} & \mathbb{1} \\ -\mathbb{1} & \boldsymbol{0} \end{pmatrix}, \quad \boldsymbol{S} := \begin{pmatrix} \boldsymbol{S}_+ & \boldsymbol{S}_2 \\ \boldsymbol{S}_2 & \boldsymbol{S}_- \end{pmatrix}, \tag{5.4}$$

where

$$(\boldsymbol{S}_\pm)_{ij} = \langle \varphi_i, \mathcal{L}_\pm \varphi_j \rangle, \quad (\boldsymbol{S}_2)_{ij} = \langle \varphi_i, \mathcal{B}\varphi_j \rangle. \tag{5.5}$$

A. Reduced eigenvalue problem: real-valued solutions

In this case one has $\mathcal{B}=0$ with

$$\mathcal{L}_+ = -\omega_{\mathrm{p}} - 3aU^2, \quad \mathcal{L}_- = -\omega_{\mathrm{p}} - aU^2, \tag{5.6}$$

where $U\epsilon^{-1/2} = x_1 q_{j,k} + y_1 q_{k,j}$ is given in Sec. IV C. Following the notation in Eq. (5.3), write

$$\varphi_1 := q_{j,k}, \quad \varphi_2 := q_{k,j}. \tag{5.7}$$

First consider the solution for which $\cos 2\varphi = 0$; i.e., Eq. (4.10). In Eq. (5.4) one then has that $\boldsymbol{S}_2 = \boldsymbol{0}$, with

$$\boldsymbol{S}_- = a\rho^2(B \pm C)\begin{pmatrix} 1 & \mp 1 \\ \mp 1 & 1 \end{pmatrix},$$

$$\boldsymbol{S}_+ = -a\rho^2\begin{pmatrix} A \pm C & \pm 3(B \pm C) \\ \pm 3(B \pm C) & A \pm C \end{pmatrix}.$$

A routine calculation then shows that the nonzero $\mathcal{O}(\epsilon)$ eigenvalue $\lambda = \lambda_1\epsilon + \mathcal{O}(\epsilon^2)$ satisfies

$$\lambda_1^2 = 2\rho^4(B \pm C)(A - 3B \mp 2C). \tag{5.8}$$

Now consider the solution that satisfies Eq. (4.11). In this case one still has $\boldsymbol{S}_2 = \boldsymbol{0}$; however, the other two submatrices now satisfy

$$\boldsymbol{S}_- = \frac{1}{2}a\rho^2\begin{pmatrix} (A-B)(1-\cos 2\varphi) & -2(B\sin 2\varphi + C) \\ -2(B\sin 2\varphi + C) & (A-B)(1+\cos 2\varphi) \end{pmatrix},$$

and

$$\boldsymbol{S}_+ = -\frac{1}{2}a\rho^2\begin{pmatrix} A + 3B + 4C\sin 2\varphi + 3(A-B)\cos 2\varphi & 6(B\sin 2\varphi + C) \\ 6(B\sin 2\varphi + C) & A + 3B + 4C\sin 2\varphi - 3(A-B)\cos 2\varphi \end{pmatrix}.$$

Another routine calculation then shows that the nonzero $\mathcal{O}(\epsilon)$ eigenvalue satisfies

$$\lambda_1^2 = -\rho^4\frac{A-B}{A-3B}(A - 3B + 2C)(A - 3B - 2C). \tag{5.9}$$

It is interesting to compare the results of Eqs. (5.8) and (5.9). In the case $C=0$, i.e., $j+k$ is odd, there is a selection mechanism defined by the quantity $A-3B$. If $A-3B>0$, then the solution defined by Eq. (4.10) has a positive $\mathcal{O}(\epsilon)$ real eigenvalue, whereas that defined by Eq. (4.11) has both $\mathcal{O}(\epsilon)$ eigenvalues being purely imaginary. The situation is reversed if $A-3B<0$. Thus, the underlying trap geometry selects the stable and unstable configurations. See Fig. 4 for a plot of $A-3B$ against V_0 for various values of (j,k). For $C\neq 0$, the selection mechanism is defined by considering the sign of the quantity $(A-3B)^2-4C^2$.

Recall that

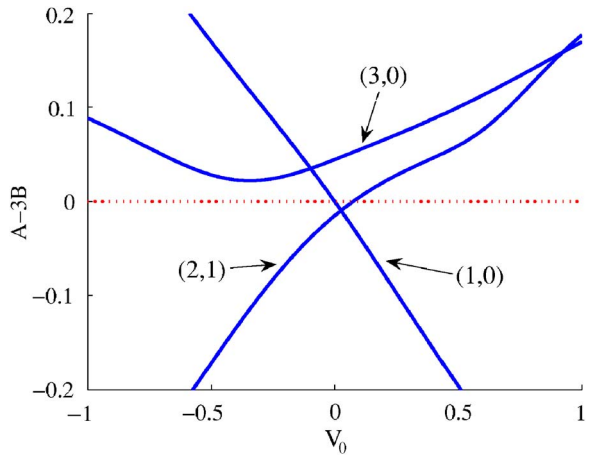

FIG. 4. (Color online) A plot of $A-3B$ vs V_0 for $p(x)=\cos 2x$, $\Omega=0.3$, and $(j,k)\in\{(1,0),(2,1),(3,0)\}$. Note that the trap geometry plays an important role in the selection of the unstable configuration.

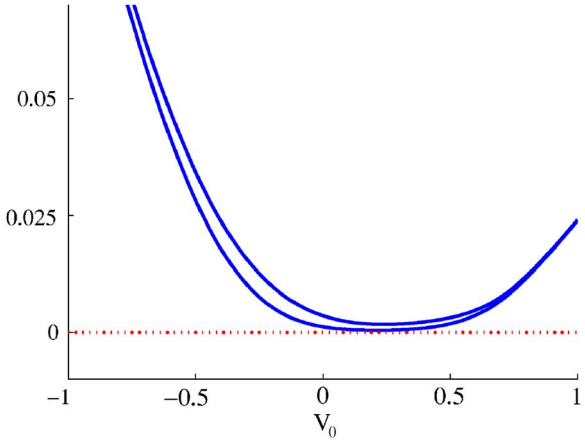

FIG. 5. (Color online) A plot of the quantities $(A-3B)^2-4C^2$ and $A^2-3AB+2C^2$ for $(j,k)=(2,0)$ and $\Omega=0.3$. Note that both quantities are positive. Since $A^2-3AB+2C^2>0$ one has $N_{\pi/4}-N_0>0$, while $(A-3B)^2-4C^2>0$ implies that the solution defined by Eq. (4.10) has a real positive $O(\epsilon)$ eigenvalue, whereas the solution defined by Eq. (4.11) has purely imaginary $O(\epsilon)$ eigenvalues.

$$N=\int\int_{\mathbb{R}^2}|q(\boldsymbol{x})|^2 d\boldsymbol{x}.$$

Let $N_{\pi/4}$ represent N for the solution given in Eq. (4.10), and let N_0 represent the solution given in Eq. (4.11). Upon using the expansion in Eq. (4.4), one sees that

$$N_{\pi/4}-N_0=\frac{(A-3B\mp 2C)^2}{A+3B\pm 4C}\frac{1}{A^2-3AB+2C^2}\epsilon+\mathcal{O}(\epsilon^{3/2}). \tag{5.10}$$

If $j+k$ is odd, then Eq. (5.10) reduces to

$$N_{\pi/4}-N_0=\frac{1}{A(A+3B)}(A-3B)\epsilon+\mathcal{O}(\epsilon^{3/2}). \tag{5.11}$$

From Eq. (5.11) and from the above analysis, one clearly sees that the nonzero $\mathcal{O}(\epsilon)$ eigenvalues are real-valued for the solution with the higher value of N. If $j+k$ is even, then the analysis is inconclusive on this point. However, in the case that $(j,k)=(2,0)$ one arrives at the same conclusion via a numerical computation of the expression in Eq. (5.10), as well as the quantity $(A-3B)^2-4C^2$ (see Fig. 5).

B. Reduced eigenvalue problem: complex-valued solutions

Let us now consider the solution given in Sec. IV D. Recalling Eq. (4.17), without loss of generality let us set $x_1=\rho$. In this case one has with

$$\mathcal{L}_+=-\omega_p-a(3U^2+V^2),\quad \mathcal{L}_-=-\omega_p-a(U^2+3V^2),$$
$$\mathcal{B}=-a2UV, \tag{5.12}$$

where $U\epsilon^{-1/2}=\rho(q_{j,k}+\cos\varphi q_{k,j})$ and $V=\rho\sin\varphi q_{k,j}$ are given in Sec. IV D. Upon setting

$$E:=\frac{B^2-C^2}{B},$$

and using Eq. (5.4) with Eq. (5.7), one eventually sees that

$$\boldsymbol{S}_-=-2a\rho^2\begin{pmatrix}E & CE/B\\ CE/B & (AE-C^2)/B\end{pmatrix},$$

$$\boldsymbol{S}_+=-2a\rho^2\begin{pmatrix}A-B+E & -CE/B\\ -CE/B & E+(A-B)C^2/B^2\end{pmatrix},$$

and

$$\boldsymbol{S}_2=2\rho^2\sin\varphi\begin{pmatrix}0 & E\\ E & -(A-B)C/B\end{pmatrix}.$$

For $C\neq 0$ the expression for the nonzero eigenvalue is too complicated to write down. However, in the case that $C=0$ one readily sees that the nonzero $\mathcal{O}(\epsilon)$ eigenvalue satisfies

$$\lambda_1^2=-4\rho^4(A^2-B^2). \tag{5.13}$$

Since $B\leqslant A$ with the inequality being generically strict, one then gets that no instabilities are generated by the $\mathcal{O}(\epsilon)$ eigenvalues.

VI. STABILITY: $\mathcal{O}(1)$ EIGENVALUES

In Sec. V the $\mathcal{O}(\epsilon)$ eigenvalues were determined. Herein we will locate the potentially unstable $\mathcal{O}(1)$ eigenvalues that arise from a Hamiltonian–Hopf bifurcation. This bifurcation is possible from the linear limit only if for the unperturbed problem there is the collision of eigenvalues of opposite sign.

Recalling the discussion in Ref. 20, Sec. IV B (also see Ref. 22, Sec. 6), we assume that the wave is such that $\omega=\lambda_{j,k}+\mathcal{O}(\epsilon)$ with $j>k$. All eigenvalues $\lambda_{m,n}\neq\lambda_{j,k}$ with $m\leqslant j$ and $n\leqslant k$ (which implies $\lambda_{m,n}<\lambda_{j,k}$) will initially map to the purely imaginary eigenvalues $\pm i(\lambda_{j,k}-\lambda_{m,n})$ with negative Krein signature, whereas those which satisfy $m\geqslant j$ and $n\geqslant k$ will map to purely imaginary eigenvalues $\pm i(\lambda_{m,n}-\lambda_{j,k})$ with positive signature. In particular, the simple eigenvalues $\lambda_{j,j}$ and $\lambda_{k,k}$ will both map to the spectral point

$$\lambda_{HH}:=i(\lambda_{j,x}-\lambda_{k,x}).$$

Thus, λ_{HH} is a semi-simple, purely imaginary eigenvalue with at least multiplicity 2; furthermore, it is a nongeneric collision of two eigenvalues with opposite Krein signature. The bifurcation associated with λ_{HH} is discussed in Ref. 22. Assuming that the multiplicity is exactly 2, the perturbed eigenvalue is given by $\lambda=\lambda_{HH}+\lambda_1\epsilon+\mathcal{O}(\epsilon^2)$, where λ_1 is an eigenvalue of the matrix $i\boldsymbol{H}/2\epsilon\in\mathbb{C}^{2\times 2}$, where

$$\boldsymbol{H}_{11}=-\langle(\mathcal{L}_++\mathcal{L}_-)q_{kk},q_{kk}\rangle,\quad \boldsymbol{H}_{22}=\langle(\mathcal{L}_++\mathcal{L}_-)q_{jj},q_{jj}\rangle,$$
$$\boldsymbol{H}_{12}=-\langle(\mathcal{L}_+-\mathcal{L}_-)q_{jj},q_{kk}\rangle-i2\langle\mathcal{B}q_{jj},q_{kk}\rangle,\quad \boldsymbol{H}_{21}=-\boldsymbol{H}_{12}^* \tag{6.1}$$

[see Eq. (5.2)].

Set

$$\Delta_{HH}:=(\boldsymbol{H}_{11}-\boldsymbol{H}_{22})^2-4|\boldsymbol{H}_{12}|^2. \tag{6.2}$$

If $\Delta_{HH}>0$, then $\lambda_1\in i\mathbb{R}$, so that no Hamiltonian–Hopf bifurcation occurs. On the other hand, if $\Delta_{HH}<0$, then $\mathrm{Re}\,\lambda_1$

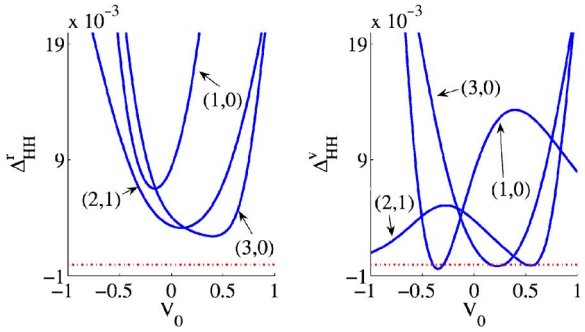

FIG. 6. (Color online) A plot of Δ^r_{HH} vs V_0 [left panel, see Eq. (6.5)] and Δ^v_{HH} vs V_0 [right panel, see Eq. (6.8)] for $p(x)=\cos 2x$, $\Omega=0.3$, and $(j,k)\in\{(1,0),(2,1),(3,0)\}$.

$\neq 0$, and a Hamiltonian–Hopf bifurcation does indeed occur. Consequently, the quantity Δ_{HH} can be used to detect these bifurcations. If the calculations support the conclusion that there is a Hamiltonian–Hopf bifurcation, then one can conclude that the wave is unstable. However, if $\Delta_{HH}>0$, then one cannot necessarily conclude that there are no other unstable eigenvalues. It may be possible that other eigenvalue collisions have occurred which have not been taken into account by this analysis (see, e.g., Ref. 22, Sec. 6).

A. Real-valued solutions

For the real-valued solutions one has $\mathcal{B}=0$, and the operators $\mathcal{L}_{\pm}$ are given in Eq. (5.6). Upon using Eq. (6.1) and the formulation given in Eq. (4.7), one eventually finds that

$$\begin{aligned}\boldsymbol{H}_{11}&=2a[\mu+2\rho^2(g_{jjkk}g_{kkkk}+\sin 2\varphi q^2_{jkkk})],\\ \boldsymbol{H}_{22}&=-2a[\mu+2\rho^2(g_{jjkk}g_{kkkk}+\sin 2\varphi q^2_{jkkk})],\\ \boldsymbol{H}_{12}&=2a\rho^2(B\sin 2\varphi+C).\end{aligned}\tag{6.3}$$

Consider the solution for which $\cos 2\varphi=0$; i.e., Eq. (4.10). After some algebraic manipulation, one sees that

$$\begin{aligned}\boldsymbol{H}_{11}-\boldsymbol{H}_{22}&=4a\rho^2[A+3B+4C\sin 2\varphi-g_{jjkk}(g_{jjjj}+g_{kkkk})\\&\quad-\sin 2\varphi(g^2_{jkkk}+g^2_{jjjk})],\\ \boldsymbol{H}_{12}&=2a\rho^2(B\sin 2\varphi+C).\end{aligned}\tag{6.4}$$

Note that in Eq. (6.4), if $C=0$, i.e., $j+k$ is odd, then

$$\begin{aligned}\boldsymbol{H}_{11}-\boldsymbol{H}_{22}&=4a\rho^2[A+3B-g_{jjkk}(g_{jjjj}+g_{kkkk})],\\ \boldsymbol{H}_{12}&=2a\rho^2B\sin 2\varphi,\end{aligned}$$

so that

$$\Delta^{\mathrm{r}}_{\mathrm{HH}}:=\frac{\Delta_{\mathrm{HH}}}{16a^2\rho^4}=[A+3B-g_{jjkk}(g_{jjjj}+g_{kkkk})]^2-B^2.\tag{6.5}$$

A plot of this quantity is given in Fig. 6. Note that for the values chosen, $\Delta^{\mathrm{r}}_{\mathrm{HH}}>0$, so that no Hamiltonian–Hopf bifurcation occurs.

Now consider the solution that satisfies Eq. (4.11). After some algebraic manipulation, one sees that

$$\begin{aligned}\boldsymbol{H}_{11}-\boldsymbol{H}_{22}&=4a\rho^2[A+C\sin 2\varphi-g_{jjkk}(g_{jjjj}+g_{kkkk})\\&\quad-\sin 2\varphi(g^2_{jkkk}+g^2_{jjjk})],\\ \boldsymbol{H}_{12}&=2a\rho^2(B\sin 2\varphi+C).\end{aligned}\tag{6.6}$$

Note in Eq. (6.6), that if $C=0$, then $\boldsymbol{H}_{12}=0$. In this case it is then straightforward to show that $\Delta_{\mathrm{HH}}>0$, so that no Hamiltonian–Hopf bifurcation occurs.

B. Complex-valued solutions

For the complex-valued solutions, the operators $\mathcal{L}_{\pm}$ and $\mathcal{B}$ are given in Eq. (5.12). Upon using the formulation in Sec. IV D, and setting without loss of generality $x_1=\rho$, one eventually sees that

$$\begin{aligned}\boldsymbol{H}_{11}-\boldsymbol{H}_{22}&=4a\rho^2[A+B-2C\cos\varphi-2g_{jjkk}(g_{jjjj}+g_{kkkk})\\&\quad-2\cos\varphi(g^2_{jkkk}+g^2_{jjjk})],\\ \boldsymbol{H}_{12}&=4a\rho^2e^{i\varphi}(B+C\cos\varphi).\end{aligned}\tag{6.7}$$

The quantity Δ_{HH} can now be computed. If $C=0$, i.e., $j+k$ is odd, then

$$\Delta^{\mathrm{v}}_{\mathrm{HH}}:=\frac{\Delta_{\mathrm{HH}}}{16a^2\rho^4}=[A+B-2g_{jjkk}(g_{jjjj}+g_{kkkk})]^2-4B^2.\tag{6.8}$$

A plot of this quantity is given in Fig. 6. Note that for each of the solutions that a Hamiltonian–Hopf bifurcation is possible if V_0 is in a band henceforth denoted as that HH vortex resonance band. Note that the geometry of the trap plays an important role in the location of such an instability band.

VII. CONCLUSIONS

In the present work we have developed a systematic framework for understanding the solutions emerging in a two-dimensional nonlinear Schrödinger equation with parabolic and periodic potentials. This study was motivated by its physical relevance in the setting of disk-shaped Bose–Einstein condensates under the combined effect of magnetic and optical trapping. We have concluded that two distinct real states and one distinct complex state can arise from each of the eigenvalues of the linear problem in this setting. Among the real states, the one with the larger norm for a fixed value of the chemical potential will generically possess a real eigenvalue pair in its linearization and hence will be exponentially unstable. The other real state will possess small imaginary eigenvalues with negative Krein signature, which may become complex upon collision with other eigenvalues of the linear spectrum. The complex solutions represent either single vortex or multivortex nonlinear bound states. These also possess negative Krein sign eigenvalues, which may or may not become complex based on conditions that depend predominantly on the nature of the geometry of the underlying linear potential.

A natural extension of the present results that appears to be tractable based on the formulation presented herein consists of the fully three-dimensional problem. To the best of our knowledge, this has not been considered in the combined presence of both parabolic and periodic potentials, although

isolated results do exist, e.g., about radially symmetric states such as the ones of Refs. 16 and 17 as well as vortex rings and related states discussed in the very recent review of Ref. 29 (see also references therein).

ACKNOWLEDGMENTS

The work of T.K. was partially supported by the NSF under Contract No. DMS-0304982 and the ARO under Contract No. 45428-PH-HSI. P.G.K. gratefully acknowledges support from NSF-CAREER, Contract Nos. NSF-DMS-0505663 and NSF-DMS-0619492.

[1]C. J. Pethick and H. Smith, *Bose-Einstein Condensation in Dilute Gases* (Cambridge University Press, Cambridge, 2001).
[2]L. Pitaevskii and S. Stringari, *Bose-Einstein Condensation* (Oxford University Press, Oxford, 2003).
[3]F. Dalfovo, S. Giorgini, L. P. Pitaevskii, and S. Stringari, Rev. Mod. Phys. **71**, 463 (1999).
[4]F. Kh. Abdullaev, A. Gammal, A. M. Kamchatnov, and L. Tomio, Int. J. Mod. Phys. B **19**, 3415 (2005).
[5]A. L. Fetter and A. A. Svidzinksy, J. Phys.: Condens. Matter **13**, R135 (2001).
[6]P. G. Kevrekidis, R. Carretero-González, D. J. Frantzeskakis, and I. G. Kevrekidis, Mod. Phys. Lett. B **18**, 1481 (2004).
[7]P. G. Kevrekidis and D. J. Frantzeskakis, Mod. Phys. Lett. B **18**, 173 (2004).
[8]C. Josserand and Y. Pomeau, Nonlinearity **14**, R25 (2001).
[9]V. Brazhnyi and V. V. Konotop, Mod. Phys. Lett. B **18**, 627 (2004).
[10]O. Morsch and M. K. Oberthaler, Rev. Mod. Phys. **78**, 179 (2006).
[11]*Emergent Nonlinear Phenomena in Bose-Einstein Condensates: Theory and Experiment*, in Springer Series on Atomic, Optical, and Plasma Physics Vol. 45, edited by P. G. Kevrekidis, D. J. Frantzeskakis, and R. Carretero-González (Springer, New York, 2008).
[12]R. Carretero-González, D. J. Frantzeskakis, and P. G. Kevrekidis, "Nonlinear waves in Bose-Einstein condensates: Physical relevance and mathematical techniques," Nonlinearity (submitted).
[13]L. Khaykovich, F. Schreck, G. Ferrari, T. Bourdel, J. Cubizolles, L. D. Carr, Y. Castin, and C. Salomon, Science **296**, 1290 (2002); K. E. Strecker, G. B. Partridge, A. G. Truscott, and R. G. Hulet, Nature (London) **417**, 150 (2002).
[14]S. Burger, K. Bongs, S. Dettmer, W. Ertmer, and K. Sengstock, Phys. Rev. Lett. **83**, 5198 (1999); J. Denschlag, J. E. Simsarian, D. L. Feder, Charles W. Clark, L. A. Collins, J. Cubizolles, L. Deng, E. W. Hagley, K. Helmerson, W. P. Reinhardt, S. L. Rolston, B. I. Schneider, and W. D. Phillips, Science **287**, 97 (2000).
[15]B. Eiermann, Th. Anker, M. Albiez, M. Taglieber, P. Treutlein, K.-P. Marzlin, and M. K. Oberthaler, Phys. Rev. Lett. **92**, 230401 (2004).
[16]Yu. S. Kivshar and T. J. Alexander, in *Proceedings of the APCTP-Nankai Symposium on Yang-Baxter Systems, Nonlinear Models and Their Applications*, edited by Q-H. Park *et al.* (World Scientific, Singapore, 1999).
[17]L. D. Carr and C. W. Clark, Phys. Rev. A **74**, 043613 (2006).
[18]G. Herring, L. D. Carr, R. Carretero-González, P. G. Kevrekidis and D. J. Frantzeskakis, Phys. Rev. A **77**, 023625 (2008).
[19]P. G. Kevrekidis, V. V. Konotop, A. Rodrigues, and D. J. Frantzeskakis, J. Phys. B **38**, 1173 (2005).
[20]T. Kapitula and P. G. Kevrekidis, Chaos **15**, 037114 (2005).
[21]I. Bloch, Nat. Phys. **1**, 23 (2005).
[22]T. Kapitula, P. G. Kevrekidis and R. Carretero-González, Physica D **233**, 112 (2007).
[23]M. Golubitsky and D. Schaeffer, *Singularities and Groups in Bifurcation Theory* (Springer, New York, 1985).
[24]T. Kapitula, P. G. Kevrekidis and B. Sandstede, Physica D **195**, 263 (2004).
[25]T. Kapitula, P. G. Kevrekidis and B. Sandstede, Physica D **201**, 199 (2005).
[26]M. Hărăguş and T. Kapitula, "On the spectra of periodic waves for infinite-dimensional Hamiltonian systems," Physica D (to be published).
[27]D. Pelinovsky and J. Yang, Stud. Appl. Math. **115**, 109 (2005).
[28]T. Kapitula, P. G. Kevrekidis, and Z. Chen, SIAM J. Appl. Dyn. Syst. **5**, 598 (2006).
[29]S. Komineas, Eur. Phys. J. Spec. Top. **147**, 133 (2007).